Soret-Dufour and Radiation Effects on Unsteady MHD Flow past an Impulsively Started Inclined Porous Plate with Variable Temperature and Mass Diffusion

N. Pandya and A. K. Shukla

***Abstract*— The objective of this paper is to investigate combined effects of Soret, Dufour and radiation on unsteady MHD flow past an impulsively started infinite inclined porous plate embedded in a porous medium with variable temperature and mass diffusion. At time $t^* > 0$ the plate moves with constant velocity u_0 and at the same time, the plate temperature and concentration levels near the plate decreased exponentially with time t^*. The governing equations of the flow field were solved numerically using Crank-Nicolson implicit finite difference method. The velocity, temperature, concentration, skin friction, Nusselt number and Sherwood number are presented through graphs and tables.**

***Keywords*—** Crank Nicolson method, Dufour effect, Heat and Mass transfer, MHD, Porous medium**.**

***MSC 2010 Codes* —76W05, 76R50, 78A40 and 76M20.**

I. INTRODUCTION

The study of unsteady free convection MHD flow with mass and heat transfer in the presence of radiation and Soret-Dufour effect has attracted a large number of mathematicians and research workers during the last many decades because of abundant avenues for research work. In astrophysics and geophysics, it is applied to study the stellar and solar structures, radio propagation through the ionosphere etc. In power engineering, the thermal physics of hydromagnetic problems with mass transfer have many applications.The unsteady free convective flow with radiation effect was investigated by Cogley et al. [1]. MHD convection flow has been studied by Cramer and Pai [2] and Raghuramal et al. [3].

If the concentration level of the fluid is low, Soret and Dufour effects are not considered otherwise ignorance of these effects is not justified. When heat and mass transfer exist simultaneously in a moving fluid, the relations between the fluxes and driving forces are of a more intricate nature. The heat flux due to mass concentration gradient is known as Dufour effect and the concentration flux due to temperature gradient is known as Soret effect.

In most of the investigation of heat and mass transfer process, it is found that Soret and Dufour effects are neglected on the behalf of smaller order of their magnitude, the effects described by Fourier and Ficks. If the density difference occurs in flow regime these effects are applicable.

Ghaly [4] analyzed the effect of radiation on heat and mass transfer over stretching sheet in the presence of a magnetic field. Raptis et al. [5] investigated the effect of radiation on two dimensional steady MHD optically thin gray gas flow along an infinite vertical plate in presence of induced magnetic field. Hady et al. [7] investigated the problem of free convection flow along a vertical wavy surface embedded in electrically conducting fluid saturated porous media in the presence of internal heat generation or absorption effect. Ganesan and Loganathan [7] investigated the radiation and mass transfer effect on flows of incompressible viscous flow past a moving vertical cylinder using Roseland approximation by the Crank-Nicolson finite difference method. Postenlnicu [8] discussed numerically the influence of a magnetic field on heat and mass transfer by natural convection from vertical surfaces in porous media with Soret and Dufour effects. Emmanuel et al. [9] investiagated numerically the effect of thermal diffusion and diffusion-thermo on combined heat and mass transfer of a steady hydromagnetic convective and slip flow due to rotating disk with viscous dissipation and ohmic heating. Karim et al. [10] investigated Dufour and Soret effect on steady MHD flow in presence of heat generation and magnetic field past an inclined stretching sheet. Sharma et al. [11] discussed Soret and Dufour effects on steady MHD convective flow past a continuously moving porous vertical plate. Very recently Bhavana et al. [12] analyzed the Soret effect on free convective unsteady MHD flow over a vertical plate with heat source.

The aim of this paper is to investigate the effects of Soret-Dufour and radiation on inclined porous plate in presence of variable temperature and concentration. The governing

N. Pandya is with the Department of Mathematics and Astronomy, Lucknow University, Lucknow - 226007, U. P., India. (phone: +91-9450397558; E-mail: dr.nidh23@gmail.com**).**
A. K. Shukla is with the Department of Mathematics and Astronomy, Lucknow University, Lucknow - 226007, U. P., India. (phone: +91-9044158184; E-mail: ashishshukla1987@gmail.com**).**

equations of flow field are solved numerically using Crank-Nicolson implicit finite difference method. The effect of different physical parameters on velocity, temperature and concentration are discussed and presented graphically.

II. Mathematical Analysis

The unsteady flow of a viscous incompressible electrically conducting fluid past an impulsively started infinite inclined porous plate with variable temperature and mass diffusion in presence of radiation is considered. The plate is inclined at angle α to vertical, is embedded in porous medium. The x^*-axis is taken along the plate and y^*-axis is taken normal to it. It is also assumed that the radiation heat flux in x^*-direction is negligible as compared to that in y^*-direction initially. The plate and fluid are at the same temperature and concentration. At time the plate is given impulsive motion along x^*-direction against gravitational field with constant velocity u_0, the plate temperature and concentration decrease exponentially with time. The transversely applied magnetic field and magnetic Reynolds number are very small and hence induced magnetic field is negligible, Cowling [13].

Due to infinite length in x^*-direction, the flow variables are functions of y^* and t^* only. Under the usual Boussinesq approximation, governing equations for this unsteady problem are given by:

Continuity equation:

$$\frac{\partial v^*}{\partial y^*} = 0 \Rightarrow v^* = -v_0 \tag{1}$$

Momentum equation:

$$\frac{\partial u^*}{\partial t^*} + v^*\frac{\partial u^*}{\partial y^*} = \nu\frac{\partial^2 u^*}{\partial y^{*2}} + g\beta(T^* - T^*_\infty)\cos(\alpha) + g\beta'(C^* - C^*_\infty)\cos(\alpha) - \frac{\sigma B_0^2 u^*}{\rho} - \frac{\nu u^*}{K^*} \tag{2}$$

Energy equation:

$$\rho C_p\frac{\partial T^*}{\partial t^*} + v^*\frac{\partial T^*}{\partial y^*} = k\frac{\partial^2 T^*}{\partial y^{*2}} - \frac{\partial q_r}{\partial y^*} + \frac{\rho D_m K_T}{c_s}\frac{\partial^2 C^*}{\partial y^{*2}} \tag{3}$$

$$\frac{\partial C^*}{\partial t^*} + v^*\frac{\partial C^*}{\partial y^*} = D\frac{\partial^2 C^*}{\partial y^{*2}} + \frac{D_m K_T}{T_m}\frac{\partial^2 T^*}{\partial y^{*2}} \tag{4}$$

where u^* and v^* is the velocity component along x^*- direction and y^*-direction respectively. g is the acceleration due to gravity, β is the volumetric coefficient of thermal expansion, β' is the coefficient of volume expansion for mass transfer, ν is the kinematic viscosity, ρ is the fluid density, B_0 is magnetic induction, K^* is the permeability of porous medium, σ is the electrical conductivity of the fluid, T^* is the dimensional temperature, T^*_∞ is temperature of free stream, C^*_∞ is concentration of free stream, D_m is the chemical molecular diffusivity, k is the thermal conductivity of the fluid , c_p is specific heat at constant pressure, K_T is thermal diffusion ratio, C^* is the dimensional concentration, q_r is radiative heat flux in y^*-direction, T_m is mean fluid temperature.

The initial and boundary conditions are:

$$\begin{aligned} &t^* \le 0 \quad u^* = 0 \quad T^* = T^*_\infty \quad C^* = C^*_\infty \quad \forall y^* \\ &t^* \ge 0 \quad u^* = u_0 \quad v^* = -v_0 \quad T^* = T^*_\infty + (T^*_\infty - T^*_\infty)\mathrm{e}^{-At^*} \\ &C^* = C^*_\infty + (C^*_w - C^*_\infty)\mathrm{e}^{-At^*} \quad at\ y^* = 0 \\ &u^* = 0 \quad T^* \to T^*_\infty \quad C^* \to C^*_\infty \quad y^* \to \infty \end{aligned} \tag{5}$$

here $A = \frac{v_0^2}{\nu}$, C^*_w and T^*_w are concentration and temperature of plate respectively.

The radiative heat flux term by using the Roseland approximation is given by

$$q_r = -\frac{4\sigma}{3k_l}\frac{\partial T^{*4}}{\partial y^*} \tag{6}$$

where k_l and σ are mean absorption coefficient and Stefan Boltzmann constant respectively. It is assumed that the temperature difference within the flow are sufficiently small such that T^{*4} may be expressed as a linear function of the temperature. This is accomplished by expanding in a Taylor series about T^*_∞ and neglecting the higher order terms, thus

$$T^{*4} \cong 4T^{*3}_\infty T^* - 3T^{*4}_\infty \tag{7}$$

then using equation (6) and (7) in equation 3 , is reduced

$$\rho C_p\frac{\partial T^*}{\partial t^*} + v^*\frac{\partial T^*}{\partial y^*} = k\frac{\partial^2 T^*}{\partial y^{*2}} + \frac{16\sigma T^{*3}_\infty}{3k_l}\frac{\partial^2 T^*}{\partial y^{*2}} + \frac{\rho D_m K_T}{c_s}\frac{\partial^2 C^*}{\partial y^{*2}} \tag{8}$$

On introducing non-dimensional quantities:

$$\begin{aligned} &u = \frac{u^*}{u_0}, t = \frac{t^* v_0^2}{\nu}, \mathrm{y} = \frac{\mathrm{y}^* v_0}{\nu}, \theta = \frac{T^* - T^*_\infty}{T^*_w - T^*_\infty}, \\ &C = \frac{\mathrm{C}^* - C^*_\infty}{\mathrm{C}^*_w - C^*_\infty}, Gm = \frac{\nu g\beta'(\mathrm{C}^*_w - \mathrm{C}^*_\infty)}{u_0 v_0^2} \\ &, Gr = \frac{\nu g\beta(\mathrm{T}^*_w - T^*_\infty)}{u_0 v_0^2}, K = \frac{v_0^2 K^*}{\nu^2}, \mathrm{Pr} = \frac{\mu c_p}{k}, \\ &M = \frac{\sigma B_0^2 \nu}{\rho v_0^2}, Du = \frac{D_m K_T(\mathrm{C}^*_w - \mathrm{C}^*_\infty)}{c_s c_p \nu(\mathrm{T}^*_w - T^*_\infty)}, Sc = \frac{\nu}{D_m}, \\ &\mathrm{Sr} = \frac{D_m K_T(\mathrm{T}^*_w - T^*_\infty)}{T_m \nu(\mathrm{C}^*_w - C^*_\infty)}, R = \frac{4\sigma T^{*3}_\infty}{k_l k} \end{aligned} \tag{9}$$

By virtue of equation (9), we get the following governing equations which are non-dimensional form of equations (2), (3) and (8) respectively

$$\frac{\partial u}{\partial t}-\frac{\partial u}{\partial y}=\frac{\partial^2 u}{\partial y^2}+Gr\cos(\alpha)\theta+Gm\cos(\alpha)\mathrm{C}-(\mathrm{M}+\frac{1}{K})\mathrm{u} \tag{10}$$

$$\frac{\partial \theta}{\partial t}-\frac{\partial \theta}{\partial y}=\frac{1}{\mathrm{Pr}}\left(1+\frac{4R}{3}\right)\frac{\partial^2 \theta}{\partial y^2}+Du\frac{\partial^2 C}{\partial y^2} \tag{11}$$

$$\frac{\partial C}{\partial t}-\frac{\partial C}{\partial y}=\frac{1}{Sc}\frac{\partial^2 C}{\partial y^2}+Sr\frac{\partial^2 \theta}{\partial y^2} \tag{12}$$

with boundary and initial condition

$$\begin{aligned} &t\le 0 \quad u=0 \quad \theta=0 \quad C=0 \quad \forall y\\ &t\ge 0 \quad u=1 \quad \theta=e^{-t} \quad C=e^{-t} \quad at \quad y=0\\ &u=0 \quad \theta\to 0 \quad C\to 0 \quad y\to\infty \end{aligned} \tag{13}$$

Skin friction: Now we calculate the non-dimensional form of skin friction (τ) from the velocity field as

$$\tau=-\left(\frac{\partial u}{\partial y}\right)_{y=0}$$

numerical values of τ are given in table-1 for different parameters.

Nusselt number: From temperature field, we study non-dimensional form of rate of heat transfer (Nu) which is given by

$$Nu=-\left(\frac{\partial \theta}{\partial y}\right)_{y=0}$$

numerical values of Nu are given in table-2 for different parameters.

Sherwood number: From concentration field, we study non-dimensional form of rate of mass transfer Sh which is given by

$$Sh=-\left(\frac{\partial C}{\partial y}\right)_{y=0}$$

numerical values of Sh are given in table-3 for different parameters.

III. Method of Solution

Equations (10)-(12) are to be solved along with their boundary and initial conditions (13) using Crank-Nicolson implicit finite difference method which is always convergent and stable. Corresponding finite difference equations for coupled partial differential equations (10)-(12) are as follows:

$$\frac{u_{i,j+1}-u_{i,j}}{\Delta t}-\frac{u_{i+1,j}-u_{i,j}}{\Delta y}$$

$$=\frac{1}{2}\left(\frac{u_{i-1,j}-2u_{i,j}+u_{i+1,j}+u_{i-1,j+1}-2u_{i,j+1}+u_{i+1,j+1}}{2(\Delta y)^2}\right)$$

$$+Gr\cos(\alpha)\left(\frac{\theta_{i,j+1}+\theta_{i,j}}{2}\right)+Gm\cos(\alpha)\left(\frac{C_{i,j+1}+C_{i,j}}{2}\right)$$

$$-\left(M+\frac{1}{K}\right)\left(\frac{u_{i,j+1}+u_{i,j}}{2}\right) \tag{14}$$

$$\frac{\theta_{i,j+1}-\theta_{i,j}}{\Delta t}-\frac{\theta_{i+1,j}-\theta_{i,j}}{\Delta y}$$

$$=\frac{1}{2\,\mathrm{Pr}}\left(1+\frac{4R}{3}\right)\left(\frac{\theta_{i-1,j}-2\theta_{i,j}+\theta_{i+1,j}+\theta_{i-1,j+1}-2\theta_{i,j+1}+\theta_{i+1,j+1}}{2(\Delta y)^2}\right)$$

$$+\frac{Du}{2}\left(\frac{C_{i-1,j}-2C_{i,j}+C_{i+1,j}+C_{i-1,j+1}-2C_{i,j+1}+C_{i+1,j+1}}{2(\Delta y)^2}\right) \tag{15}$$

$$\frac{C_{i,j+1}-C_{i,j}}{\Delta t}-\frac{C_{i+1,j}-C_{i,j}}{\Delta y}$$

$$=\frac{1}{2Sc}\left(\frac{C_{i-1,j}-2C_{i,j}+C_{i+1,j}+C_{i-1,j+1}-2C_{i,j+1}+C_{i+1,j+1}}{2(\Delta y)^2}\right)$$

$$+\frac{Sr}{2}\left(\frac{\theta_{i-1,j}-2\theta_{i,j}+\theta_{i+1,j}+\theta_{i-1,j+1}-2\theta_{i,j+1}+\theta_{i+1,j+1}}{2(\Delta y)^2}\right) \tag{16}$$

corresponding boundary condition

$$\begin{aligned} &u_{i,0}=0, \quad \theta_{i,0}=0, \quad C_{i,0}=0 \quad \forall i\\ &u_{0,\mathrm{j}}=1, \quad \theta_{0,\mathrm{j}}=e^{-j\Delta t}, \quad C_{0,\mathrm{j}}=e^{-j\Delta t}\\ &u_{\mathrm{L,j}}=0, \quad \theta_{\mathrm{L,j}}\to 0, \quad C_{\mathrm{L,j}}\to 0 \end{aligned} \tag{17}$$

here, index i refers to y and j refers to time. Also $\Delta t=t_{j+1}-t_j$ and $\Delta y=y_{i+1}-y_i$ knowing the values of u,θ and C at a time t, we can calculate the values at a time $t+\Delta t$ as follows we substitute $i=1,2,3,\cdots\cdots \mathrm{L}-1$ in equations (14)-(16) which constitute a tridiagonal system of equations, can be solved by Thomas algorithm as discussed in Carnahan et al. [14]. Thus θ and C are known for all values of y at $t+\Delta t$. Substitute these values of θ and C in equation (14) and solved by same procedure with initial and boundary condition, we obtain solution for u till desired time t.

IV. Result and Discussion

In order to get insight into the physical problem, numerical results for non-dimensional velocity field u, temperature field θ and concentration field C are displayed with the help of graphs by assigning numerical values of magnetic parameter M, thermal Grashof number Gr, the solutal Grashof number Gm, Prandtl number Pr, Schmidt number Sc, radiation parameter R, Soret number Sr, Dufour number Du, permeability of porous medium K and inclination angle α.

Figures 1 to 11 depict the variation of dimensionless velocity field u against the influence of physical parameters. Figures 1 to 4 demonstrate the effect of Prandtl number Pr,

magnetic parameter M, inclination angle α and Schmidt number Sc over the velocity field u. It is to be noted that Schmidt number is the ratio of kinematic viscosity with molecular diffusivity. Prandtl number is the ratio of viscous force to the thermal force. When Pr, M, Sc increase, velocity decrease along with other parameters are fixed and also inclination angle increase, it is seen velocity decreases as α increases, the effect of the buoyancy force decreases because of multiplication factor $cos(\alpha)$.

For different values of radiation parameter R, permeability K and Grashof number Gr, the velocity field are plotted in figures 5 to 7. It is seen that velocity increases as these parameters increase. Increasing solutal Grashof number Gm, the Soret number Sr and Dufour number Du , increases velocity of flow field as seen in figures 8 to 10. The influence of time t on velocity field illustrated in figure 11. It is seen that near the wall velocity increases rapidly as time increases.
Figures 12 and 13 depict that temperature decreases as Prandtl number Pr and Soret number Sr increases and increasing the Schmidt number Sc and Dufour number Du, increases temperature of flow field as seen in figures 14 and 15. Figure 16 reveals that temperature increases as radiation parameter R increases.

Figure 17 shows that the fluid concentration C, first increase rapidly then decrease on increasing Prandtl number Pr. For different values of Dufour number concentration field are displayed in figure 18. It is observed that concentration increases first near the wall as Du increases and far some distance from wall concentration decreases as Du increase. Figure 19 depicts that on increases Soret number Sr, concentration increases

Increasing Schmidt number Sc, it is analyzed that concentration field decreases in figure 20. This causes the concentration buoyancy effects to decrease yielding a reduction in the fluid velocity. It is analyzed in figure 21 that on increasing radiation parameter R, concentration decreases.

Table-1 displays the variation of skin friction against different parameters. It is observed that on increasing Schmidt number Sc, Prandtl number Pr, magnetic parameter M and inclination angle α, skin friction coefficient τ increases. And on increasing Soret number Sr, radiation parameter R, Dufour number Du, solutal Grashof number Gm, Grashof number Gr, permeability K and time t, skin friction coefficient τ decreases.

Table-2 displays that on increasing Soret number, Prandtl number and Dufour number, Nusselt number (Nu) inceases. And on increasing Schmidt number, radiation parameter R and time, Nusselt number decreases.

Table-3 shows that on increasing Schmidt number and radiation parameter Sherwood number (Sh) increases. And on increasing Soret number, Prandtl number, Dufour number and time, Sherwood number decreases.

V. CONCLUSION

In this paper we have studied Soret-Dufour and radiation effects on MHD flow past an impulsively started inclined porous plate embedded in porous medium. From present numerical study the following conclusion can be drawn:

1. The velocity decreases with increase in inclination angle.
2. The velocity increases with increase in Soret number.
3. The concentration decreases with increase in Schmidt number.
4. The temperature is observed to increase with an increase Schmidt number Sc.
5. The concentration increases with increase in Prandtl number Pr.
6. Skin friction coefficient decreases, Nusselt number increases and Sherwood number decreases when Soret number increases.
7. Skin friction coefficient decreases, Nusselt number increases and Sherwood number decreases when Dufour number increases.
8. Skin friction coefficient increases when inclination angle increases.

ACKNOWLEDGMENT

We acknowledge the U.G.C. (University Grant Commission) and thank for providing financial support for the research work. We are also thankful to different software/hardware companies (Mathematica, Microsoft, Matlab etc.) for developing the techniques that help in the computation and editing.

REFERENCES

1. A.C. Cogley, W.C. Vincenti and S.E. Gilles, "Differential approximation for radiation transfer in a non-gray gas near equilibrium," *Am. Inst. Aeronaut Astronaut J.*, vol. 6, pp. 551-555, 1968.
2. K.P. Cramer and S.I.. Pai, *Magneto fluid dynamics for engineering and applied physics*, McGraw Hills book co., NewYork, 1973.
3. B. Rajesh Kumar, D.R.S. Raguraman, R. Muthucumareswamy, "Hydromagnetic flow and heat transfer on a continuous moving vertical surface," *Acta Mech*., vol. 155, pp. 249-253, 2002.
4. A.Y. Ghly, "Radiation effect on a certain MHD free convection flow," *Chaos, Solution and Fractals*, vol. 13(9), pp. 1843-1850, 2002.
5. A. Raptis, C. Perdikis and A. Leontitsis, "Effect of radiation in an optically thin gray gas flowing past a vertical infinite plate in presence of a magnetic field," *Heat and Mass Transfer*, vol. 39, pp. 771-773, 2003.
6. F. M Hady, R.A. Mohamed and A. Mahdy, "A MHD free convection flow along a vertical wavy surface with heat generation or absorption effect," *Int. Comm. Heat Mass Transfer*, vol. 33, pp. 1253-1263, 2006.
7. P. Ganesan and P. Laganathan, "Radiation and Mass transfer effects on flow of an incompressible viscous fluid past a moving sylinder," *Int. J. of Heat and Mass Transfer*, vol. 45, pp. 4281-4288, 2002.
8. A. Postelnicu, "Influence of a magnetic field on heat and mass transfer by natural convection from vertical surfaces in porous media considering Soret and Dufour effects," *Int. J. of Heat and Mass Transfer*, vol. 47(6-7), pp. 1467-1472, 2004.
9. Osalusi Emmanuel, Side Jonathan and Harris Robert, "Thermal diffusion an diffusion thermo effects on combined heat and mass transfer on a steady MHD convective and slip flow due to rotating disk with viscous dissipation and ohmic heating," *Int. Comm. In Heat and Mass Transfer*, vol. 35, pp. 908-905, 2008.
10. M D Enamul Karim, M D Abdus Samad and M D Maruf Hasan, "Dufour and Soret effect on steady MHD flow in presence of Heat generation and magnetic field past an inclined stretching sheet," *Open Journal of Fluid Dynamics,* vol. 2, pp. 91-100, 2012.

11. Dipak Sharma, Nazibuddin Ahmed and Pulak Kr Mahanta, "Soret and Dufour effects on steady MHD convective flow past a continuously moving porous vertical plate," *Int. J. of Eng. Sci. and Tech*., vol 4, no. 12, pp. 4757-4765, 2012.
12. M. Bhavana, D. Chenna Kesaraiah and A. Sudhakarraiah, "The Soret effect on free convective unsteady MHD flow over a vertical plate with heat source," *Int. J. of Innovative R. in Sci. Eng. And Tech*., vol. 2(5), pp. 1617-1628, 2013.
13. T.G. Cowling, *Magnetohydrodynamics*, Inter Science Publishers, NewYork, 1957.
14. H.A. Carnahan , J.O. Luthorand and Wilkes, *Applied Numerical Methods*, John Wiley & Sons, NewYork, 1969

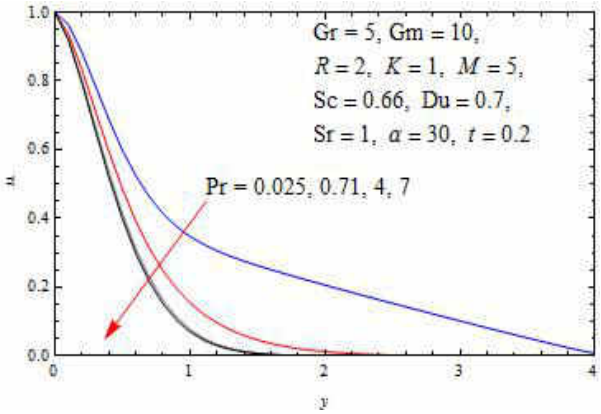

Figure 1: Velocity Profile for different values of Pr

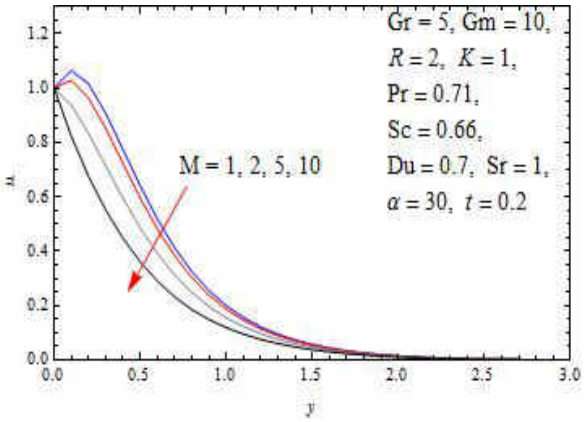

Figure 2: Velocity Profile for different values of M

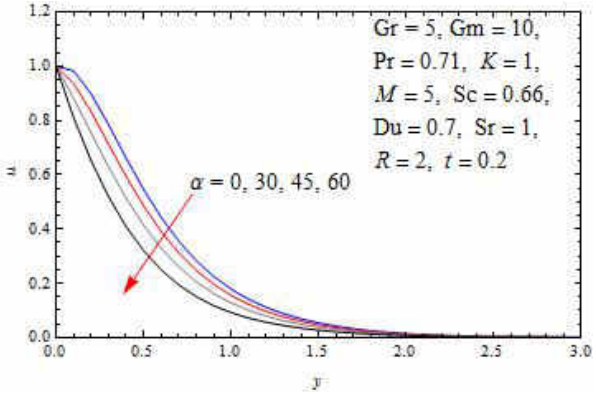

Figure 3: Velocity Profile for different values of α

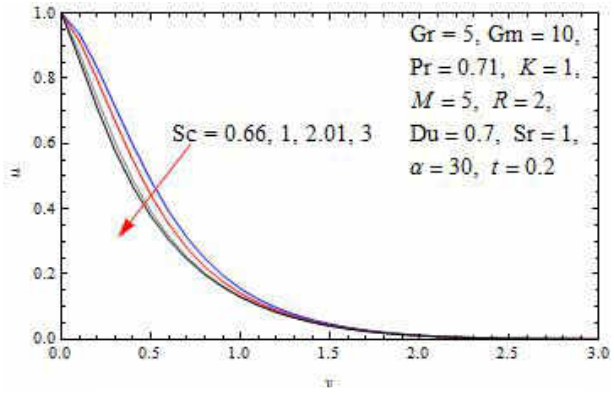

Figure 4: Velocity Profile for different values of Sc

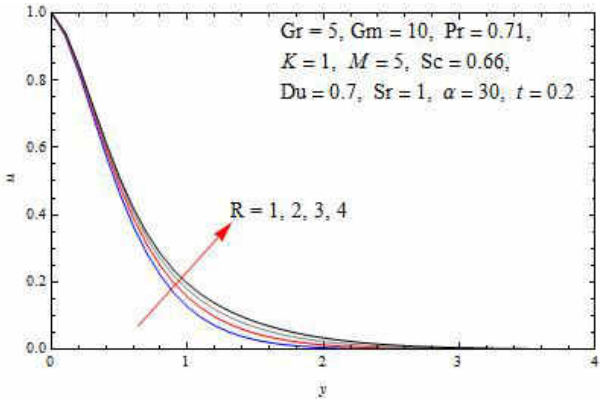

Figure 5: Velocity Profile for different values of R

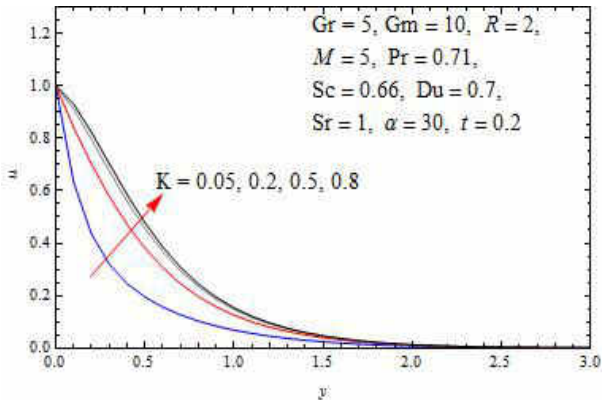

Figure 6: Velocity Profile for different values of K

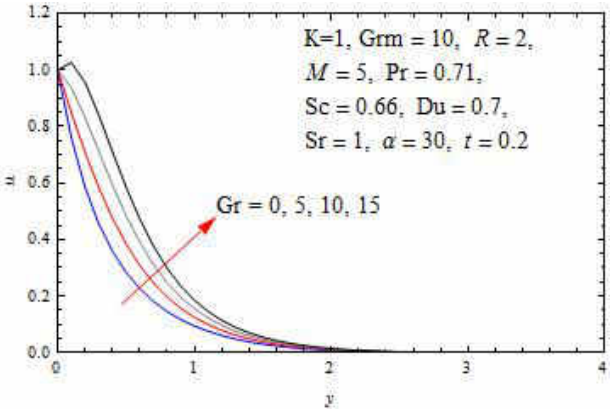

Figure 7: Velocity Profile for different values of Gr

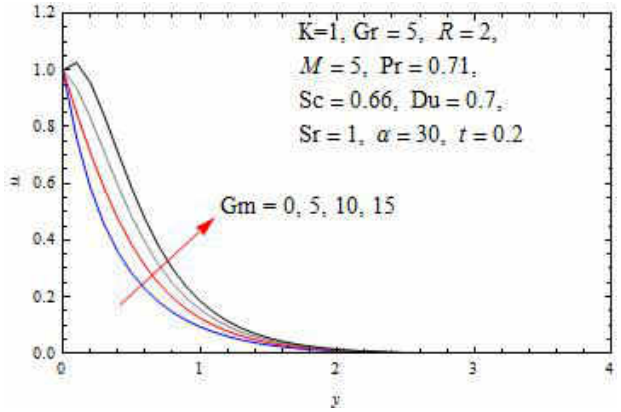

Figure 8: Velocity Profile for different values of Gm

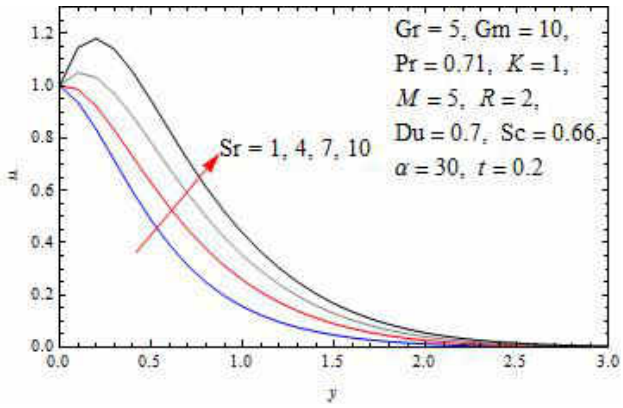

Figure 9: Velocity Profile for different values of Sr

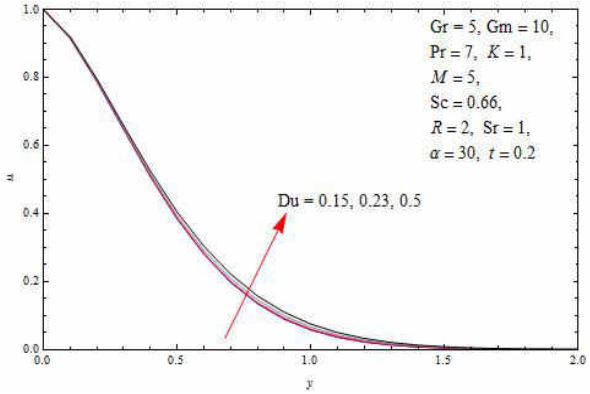

Figure10: Velocity Profile for different values of Du

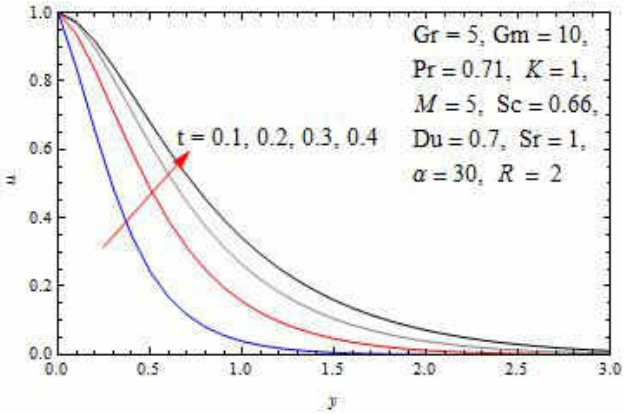

Figure 11: Velocity Profile for different values of t

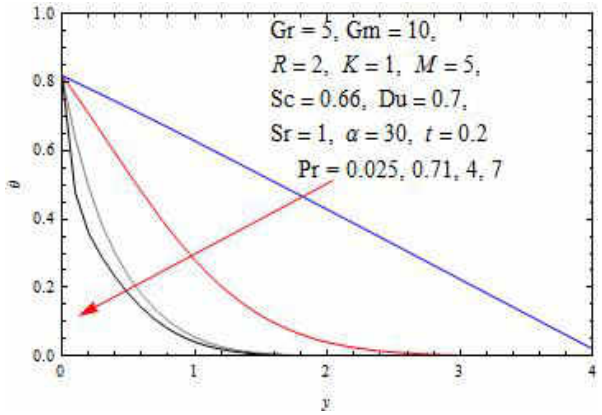

Figure 12: Temperature Profile for different values of Pr

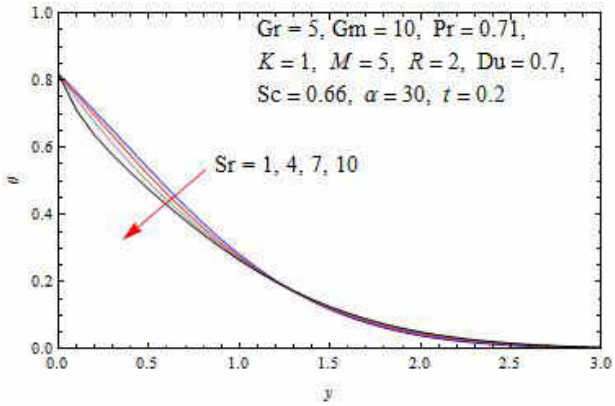

Figure 13: Temperature Profile for different values of Sr

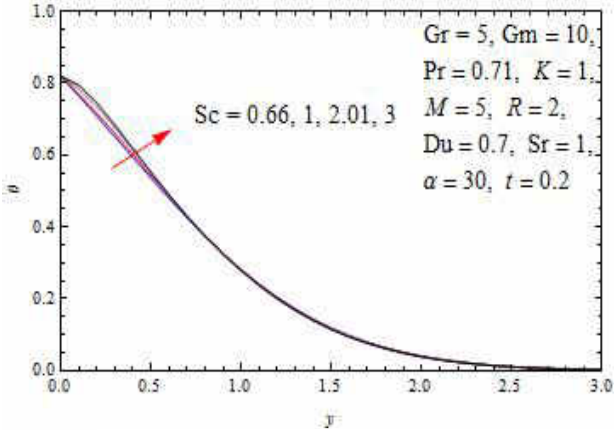

Figure 14: Temperature Profile for different values of Sc

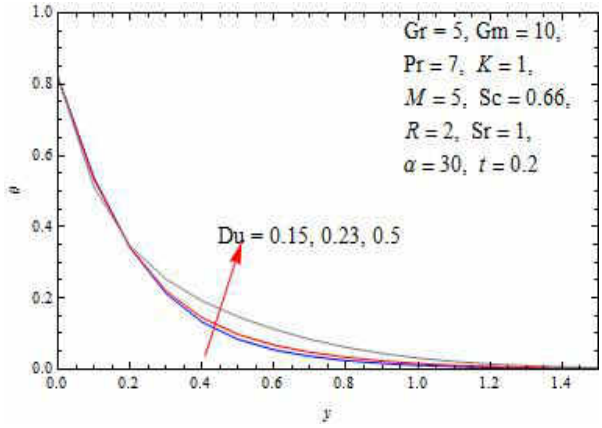

Figure 15: Temperature Profile for different values of Du

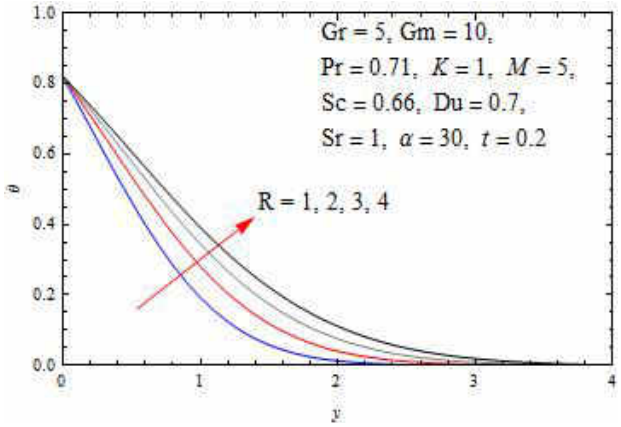

Figure 16: Temperature Profile for different values of R

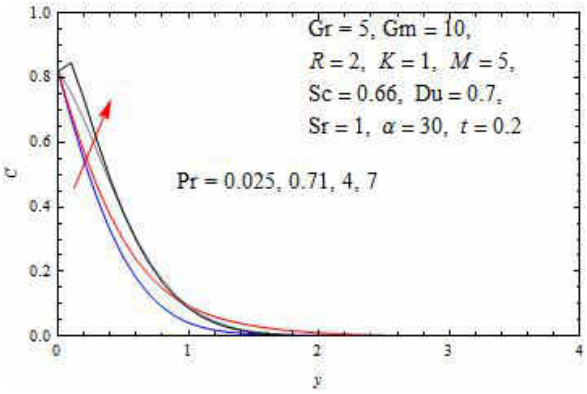

Figure 17: Concentration Profile for different values of Pr

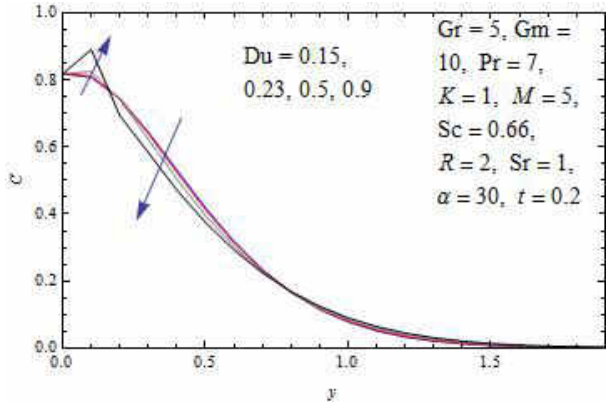

Figure 18: Concentration Profile for different values of Du

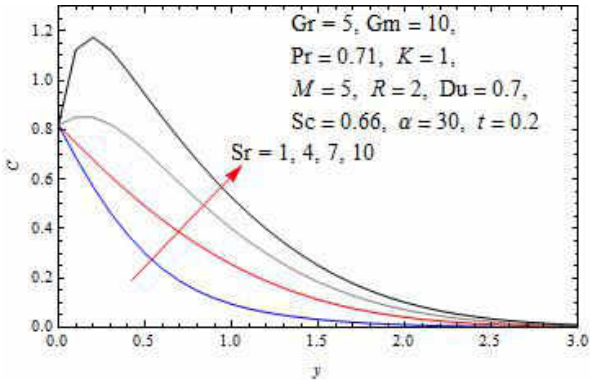

Figure 19: Concentration Profile for different values of Sr

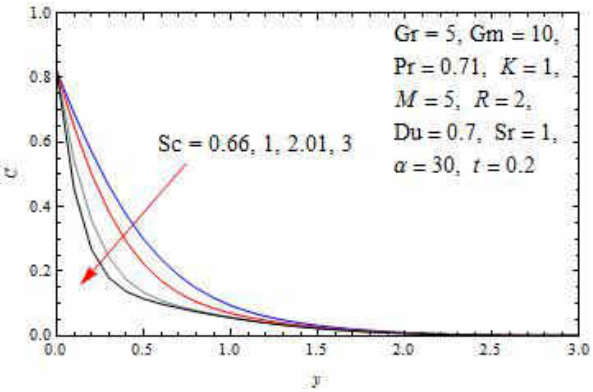

Figure 20: Concentration Profile for different values of Sc

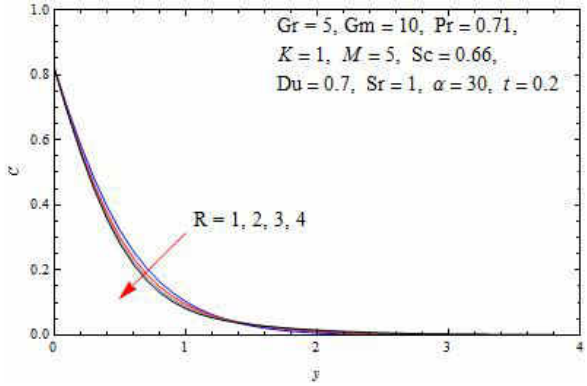

Figure 21: Concentration Profile for different values of R

Table-1 Skin friction coefficient for different values of parameters

t	R	Pr	M	K	Sc	Sr	α	Du	Gm	Gr	τ
0.2	1	0.71	5	1	0.66	1	30	0.7	10	5	0.677699
0.2	2	0.71	5	1	0.66	1	30	0.7	10	5	0.596546
0.2	4	0.71	5	1	0.66	1	30	0.7	10	5	0.570962
0.2	2	0.025	5	1	0.66	1	30	0.7	10	5	0.362564
0.2	2	4	5	1	0.66	1	30	0.7	10	5	0.789139
0.2	2	7	5	1	0.66	1	30	0.7	10	5	0.819804
0.2	2	0.71	1	1	0.66	1	30	0.7	10	5	-0.637714
0.2	2	0.71	2	1	0.66	1	30	0.7	10	5	-0.282283
0.2	2	0.71	10	1	0.66	1	30	0.7	10	5	1.77518
0.2	2	0.71	5	0.1	0.66	1	30	0.7	10	5	3.67869
0.2	2	0.71	5	0.2	0.66	1	30	0.7	10	5	1.57543
0.2	2	0.71	5	0.5	0.66	1	30	0.7	10	5	0.89147
0.2	2	0.71	5	0.8	0.66	1	30	0.7	10	5	0.697203
0.2	2	0.71	5	1	1	1	30	0.7	10	5	0.848431
0.2	2	0.71	5	1	2.01	1	30	0.7	10	5	1.21819
0.2	2	0.71	5	1	3	1	30	0.7	10	5	1.42273
0.2	2	0.71	5	1	0.66	4	30	0.7	10	5	0.137321
0.2	2	0.71	5	1	0.66	7	30	0.7	10	5	-0.501332
0.2	2	0.71	5	1	0.66	10	30	0.7	10	5	-1.45397
0.2	2	0.71	5	1	0.66	1	0	0.7	10	5	0.170335
0.2	2	0.71	5	1	0.66	1	45	0.7	10	5	1.17542
0.2	2	0.71	5	1	0.66	1	60	0.7	10	5	1.88612
0.2	2	7	5	1	0.66	1	60	0.15	10	5	0.853805
0.2	2	7	5	1	0.66	1	60	0.23	10	5	0.849171
0.2	2	7	5	1	0.66	1	60	0.5	10	5	0.832853
0.2	2	7	5	1	0.66	1	60	0.9	10	5	0.805094
0.2	1	0.71	5	1	0.66	1	30	0.7	0	5	2.39812
0.2	1	0.71	5	1	0.66	1	30	0.7	5	5	1.5141
0.2	1	0.71	5	1	0.66	1	30	0.7	15	5	-0.253943
0.2	1	0.71	5	1	0.66	1	30	0.7	10	0	1.83387
0.2	1	0.71	5	1	0.66	1	30	0.7	10	10	-0.57371
0.2	1	0.71	5	1	0.66	1	30	0.7	10	15	-1.7775
0.1	2	0.71	5	1	0.66	1	30	0.7	10	5	1.61605
0.3	2	0.71	5	1	0.66	1	30	0.7	10	5	0.31741
0.4	2	0.71	5	1	0.66	1	30	0.7	10	5	0.263876

Table-2 Nusselt number for different values of parameters

t	R	Pr	M	K	Sc	Sr	α	Du	Gm	Gr	Nu
0.2	1	0.71	5	1	0.66	1	30	0.7	10	5	0.713983
0.2	2	0.71	5	1	0.66	1	30	0.7	10	5	0.457699
0.2	4	0.71	5	1	0.66	1	30	0.7	10	5	0.401949
0.2	2	0.025	5	1	0.66	1	30	0.7	10	5	0.184299
0.2	2	4	5	1	0.66	1	30	0.7	10	5	1.8278
0.2	2	7	5	1	0.66	1	30	0.7	10	5	3.40565
0.2	2	0.71	5	1	1	1	30	0.7	10	5	0.493258
0.2	2	0.71	5	1	2.01	1	30	0.7	10	5	0.358525
0.2	2	0.71	5	1	3	1	30	0.7	10	5	0.244963
0.2	2	0.71	5	1	0.66	4	30	0.7	10	5	0.615553
0.2	2	0.71	5	1	0.66	7	30	0.7	10	5	0.743868
0.2	2	0.71	5	1	0.66	10	30	0.7	10	5	1.09003
0.2	2	7	5	1	0.66	1	30	0.15	10	5	2.8126
0.2	2	7	5	1	0.66	1	30	0.23	10	5	2.85447
0.2	2	7	5	1	0.66	1	30	0.5	10	5	3.07542
0.2	2	7	5	1	0.66	1	30	0.9	10	5	4.17995
0.1	2	0.71	5	1	0.66	1	30	0.7	10	5	0.892766
0.3	2	0.71	5	1	0.66	1	30	0.7	10	5	0.377694
0.4	2	0.71	5	1	0.66	1	30	0.7	10	5	0.272914

Table-3 Sherwood number for different values of parameters

t	R	Pr	M	K	Sc	Sr	α	Du	Gm	Gr	Sh
0.2	1	0.71	5	1	0.66	1	30	0.7	10	5	1.2275
0.2	2	0.71	5	1	0.66	1	30	0.7	10	5	1.34024
0.2	4	0.71	5	1	0.66	1	30	0.7	10	5	1.36174
0.2	2	0.025	5	1	0.66	1	30	0.7	10	5	1.44484
0.2	2	4	5	1	0.66	1	30	0.7	10	5	0.636429
0.2	2	7	5	1	0.66	1	30	0.7	10	5	-0.264777
0.2	2	0.71	5	1	1	1	30	0.7	10	5	1.72041
0.2	2	0.71	5	1	2.01	1	30	0.7	10	5	2.77515
0.2	2	0.71	5	1	3	1	30	0.7	10	5	3.65456
0.2	2	0.71	5	1	0.66	4	30	0.7	10	5	0.715816
0.2	2	0.71	5	1	0.66	7	30	0.7	10	5	-0.32508
0.2	2	0.71	5	1	0.66	10	30	0.7	10	5	-3.04477
0.2	2	7	5	1	0.66	1	30	0.15	10	5	0.0989752
0.2	2	7	5	1	0.66	1	30	0.23	10	5	0.0722786
0.2	2	7	5	1	0.66	1	30	0.5	10	5	-0.0649134
0.2	2	7	5	1	0.66	1	30	0.9	10	5	-0.725551
0.1	2	0.71	5	1	0.66	1	30	0.7	10	5	1.93473
0.3	2	0.71	5	1	0.66	1	30	0.7	10	5	0.986633
0.4	2	0.71	5	1	0.66	1	30	0.7	10	5	0.780744